Published in final edited form as:
Cancer Cell. 2009 July 7; 16(1): 21–32. doi:10.1016/j.ccr.2009.04.012.

AKT-independent signaling downstream of oncogenic *PIK3CA* mutations in human cancer

Krishna M. Vasudevan[1,2,3,*], **David A. Barbie**[1,4,11,*], **Michael A. Davies**[6,*], **Rosalia Rabinovsky**[1,2,3], **Chontelle J. McNear**[1,2], **Jessica J. Kim**[1,2], **Bryan T. Hennessy**[6], **Hsiuyi Tseng**[1], **Panisa Pochanard**[1], **So Young Kim**[1,2,4], **Ian F. Dunn**[1,2,3,4], **Anna C. Schinzel**[1,2,4], **Peter Sandy**[7], **Sebastian Hoersch**[7], **Qing Sheng**[1,3], **Piyush B. Gupta**[4], **Jesse S. Boehm**[4], **Jan H. Reiling**[8], **Serena Silver**[4], **Yiling Lu**[6], **Katherine Stemke-Hale**[6], **Bhaskar Dutta**[6], **Corwin Joy**[6], **Aysegul A. Sahin**[6], **Ana Maria Gonzalez-Angulo**[6], **Ana Lluch**[9], **Lucia E. Rameh**[10], **Tyler Jacks**[7], **David E. Root**[4], **Eric S. Lander**[4], **Gordon B. Mills**[6], **William C. Hahn**[1,2,3,4], **William R. Sellers**[1,5], and **Levi A. Garraway**[1,2,3,4,†]

[1]Department of Medical Oncology, Dana-Farber Cancer Institute, Harvard Medical School, Boston, MA 02115, USA.

[2]Center for Cancer Genome Discovery, Dana-Farber Cancer Institute, Harvard Medical School, Boston, MA 02115, USA.

[3]Departments of Medicine and Neurosurgery, Brigham and Women's Hospital, Harvard Medical School, Boston, MA 02115, USA

[4]The Broad Institute of M.I.T. and Harvard, 7 Cambridge Center, Cambridge, MA 02142, USA.

[5]Novartis Institutes for BioMedical Research, 250 Massachusetts Avenue, Cambridge, MA 02139, USA.

[6]Department of Systems Biology, University of Texas, M.D. Anderson Cancer Center, Houston, TX 77030, USA

[7]Koch Institute for Integrative Cancer Research, Massachusetts Institute of Technology, 77 Massachusetts Avenue, Cambridge, MA 02139, USA

[8]Whitehead Institute for Biomedical Research, 9 Cambridge Center Cambridge, MA 02142 USA

[9]Universidad de Valencia Clinic Hospital, Valencia, Spain

†To whom correspondence should be addressed: Levi A. Garraway Phone: 617−632−6689 Fax: 617−632−6689 Email: levi_garraway@dfci.harvard.edu.
*These authors contributed equally to this work.

SIGNIFICANCE

Genetic alterations targeting the PI3 kinase pathway are highly prevalent in many human cancers. For example, gain-of-function mutations in *PIK3CA*, which encodes a key enzymatic subunit of PI3 kinase, occur frequently in breast, colon, and endometrial cancers, among others. Downstream activation of the AKT kinase is regarded as the dominant tumor-promoting mechanism enacted by PI3 kinase signaling. However, this study shows that AKT signaling is markedly diminished in many cancer cell lines and human breast tumors harboring *PIK3CA* mutations. Instead, these cells elaborate a signaling pathway involving the PI3 kinase effector PDK1 and its downstream substrate SGK3. These findings may have important implications for PI3 kinase signaling and the development of rational therapeutics against this key cancer pathway.

Supplemental Data

Supplemental Data accompanies this paper.

[10]Boston Biomedical Research Institute, 64 Grove Street, Watertown, MA 02472, USA

[11]Massachusetts General Hospital Cancer Center, 55 Fruit Street, Boston, MA 02114, USA.

Summary

Dysregulation of the phosphatidylinositol 3-kinase (PI3K) signaling pathway occurs commonly in human cancer. *PTEN* tumor suppressor or *PIK3CA* oncogene mutations both direct PI3K-dependent tumorigenesis largely through activation of the AKT/PKB kinase. However, here we show through phospho-protein profiling and functional genomic studies that many *PIK3CA*-mutant cancer cell lines and human breast tumors exhibit only minimal AKT activation, and a diminished reliance on AKT for anchorage-independent growth. Instead, these cells retain robust PDK1 activation and membrane localization, and exhibit dependency on the PDK1 substrate SGK3. SGK3 undergoes PI3K- and PDK1-dependent activation in *PIK3CA*-mutant cancer cells. Thus, PI3K may promote cancer through both AKT-dependent and AKT-independent mechanisms. Knowledge of differential PI3K/PDK1 signaling could inform rational therapeutics in cancers harboring *PIK3CA* mutations.

Keywords

PI3 kinase; PTEN; AKT; PDK1; SGK3; cancer

Introduction

Dysregulation of the phosphatidylinositol 3-kinase (PI3K) signaling pathway occurs commonly in cancer (Vivanco and Sawyers, 2002). Upon activation at the plasma membrane by receptor tyrosine kinases or RAS proteins (Engelman et al., 2006), PI3Ks phosphorylate the D3 position on membrane phosphatidylinositides, thereby recruiting and activating proteins that contain a pleckstrin homology (PH) or other lipid-binding domain. This activity is antagonized by the PTEN tumor suppressor protein. The serine/threonine kinase AKT/PKB (AKT), upon activation by PDK1 and the TORC2 complex (Alessi et al., 1997; Sarbassov et al., 2005; Stephens et al., 1998), is believed to transduce the major downstream PI3K signal in cancer. AKT regulates cell growth and survival pathways by phosphorylating substrates such as GSK3, Forkhead transcription factors, and the TSC2 tumor suppressor protein (Vivanco and Sawyers, 2002).

Both *PTEN* and *PIK3CA*, which encodes the catalytic (p110α) subunit of P13K, are frequently mutated across many human cancers. The most common tumor-associated *PIK3CA* mutations (>80% of cases) involve either the helical domain (exon 9; e.g., E542K and E545K) or the kinase domain (exon 20; e.g., H1047R) of p110α (Samuels et al., 2004, Samuels et al., 2005). Inactivating *PTEN* mutations occur commonly in prostate cancer, endometrial cancer, and glioblastoma, among others (Vivanco and Sawyers, 2002). Rare activating somatic mutations of *AKT1* have also been described in cancer (Carpten et al., 2007).

Although inactivating PTEN mutations and activating *PIK3CA* mutations both augment AKT signaling in several experimental systems (Kang et al., 2005; Nakamura et al., 2000), it is not clear whether such genetic alterations are functionally redundant in vivo. For example, in endometrial cancers *PIK3CA* and *PTEN* mutations often co-occur (Oda et al., 2005), suggesting that they may have distinct roles. Similarly, *PIK3CA* mutations may be seen in breast cancers with low PTEN levels, and AKT phosphorylation correlates poorly with *PIK3CA* mutation in this malignancy (Stemke-Hale et al., 2008). In addition, while PTEN loss has been associated with adverse clinical outcome in breast cancer (Depowski et al., 2001), the prognosis associated with *PIK3CA* alterations may depend on the type of mutation. In one study, for example, helical mutations correlated with poorer prognosis than kinase-domain mutations (Barbareschi et al.,

2007). Thus, as observed for RAS and RAF oncoproteins in the MAP kinase cascade (Solit et al., 2006), the position of somatic alterations within the PI3K pathway (or *PIK3CA* itself) may influence the mechanisms and, by extension, the functional output of oncogenic pathway deregulation. Here, we employed a phospho-protein profiling and functional genetic approach to characterize signaling mechanisms downstream of PI3K in *PIK3CA*-mutant cancer cells.

Results

PIK3CA-mutant cancer cells frequently show diminished AKT signaling

To determine whether somatic PTEN loss and *PIK3CA* activation lead to the same signaling consequences in cancer, we interrogated phospho-protein profiles associated with distinct alterations affecting the PI3K pathway by reverse-phase protein array (RPPA) analysis (Tibes et al., 2006). Analysis of the quantitative protein expression signal from PTEN and phosphorylated AKT (p-AKT) in the NCI60 cancer cell line collection (Stinson et al., 1992) identified 12 lines with low or absent PTEN protein (Figure 1A). As expected (Nakamura et al., 2000), all cell lines with low PTEN (PTEN-null) exhibited enhanced AKT phosphorylation (p-AKT) at both serine 473 and threonine 308 (Figures 1B and 1C; $p < 0.001$ for both p-AKT sites).

We then analyzed the relationship between the *PIK3CA* mutations and levels of p-AKT. Previous sequencing studies identified 7 NCI60 cell lines (spanning four tumor types) that harbor *PIK3CA* mutations; 3 lines with kinase-domain mutations (SK-OV-3, HCT-116, and T-47D), and 4 with helical mutations (HT-29, HCT-15, MCF-7, and NCI-H460) (http://www.sanger.ac.uk/genetics/CGP/cosmic/; and confirmed with the lines used here). In contrast to the PTEN-null setting, NCI60 lines with activating *PIK3CA* mutations contained much lower p-AKT RPPA signals when compared to PTEN-null cell lines, irrespective of tumor type ($p < 0.001$ for Ser473 and $p = 0.002$ for Thr308; Figures 1B and 1C).

As *PIK3CA* mutations were relatively uncommon in the NCI60 panel, we confirmed this observation in 51 human breast cancer cell lines (Neve et al., 2006) (Figure S1). We also observed similar RPPA patterns by hierarchical clustering of PTEN and p-AKT RPPA signals in 64 hormone receptor-positive breast tumor samples (Figure S2). Whereas elevated p-AKT at Ser473 and Thr308 correlated inversely with PTEN levels in all cases, many *PIK3CA*-mutant cell lines and breast tumors contained low p-AKT levels (Figures S1, S2). In these experiments, reduced p-AKT expression was particularly apparent (though not universal) in the setting of helical (e.g., E542K/E545K) *PIK3CA* mutations (*PIK3CA*^{helical}) (Figures S1B, S1C, and S2B), although multiple cell lines and tumors with kinase domain (e.g., H1047R) mutations (*PIK3CA*^{kinase}) also showed low p-AKT (Figures 1B, 1C, S1B, S1C, and S2A). These findings, together with previous studies of human breast tumors (Stemke-Hale et al., 2008), raised the possibility that PTEN loss and *PIK3CA* mutation might have different effects on AKT signaling.

To examine AKT pathway activation in more detail, we performed immunoblot analyses on selected cancer cell lines that lack *PTEN* or express activating *PIK3CA* alleles. Strikingly, p-AKT at both Ser473 and Thr308 was markedly diminished in the four *PIK3CA*^{helical} cell lines examined, as shown in Figure 1D. AKT phosphorylation in *PIK3CA*^{kinase} cells was more variable, approaching the levels observed in PTEN-null cells in some cases (e.g., BT-20, MDA-MB-453, and HCC1954; Figure 1D), while virtually undetectable in others (e.g., HCT-116; Figure S3A). For most ensuing experiments, we considered MCF-7, HCT-15, and SW948 as representative *PIK3CA*-mutant cells with low p-AKT; T47D and HCC1954 as representative *PIK3CA*-mutant cell lines with elevated p-AKT; and 786−0 as a representative PTEN-null cell line. Additional studies under serum-starved conditions showed that the level of AKT phosphorylation in several *PIK3CA*-mutant cancer cell lines was comparable to a non-

transformed setting (e.g., MCF-10A and MCF-12A cells; Figure S3B). Thus, many *PIK3CA*-mutant cancer cells exhibited unexpectedly low AKT signaling.

We considered the possibility that the reduced AKT phosphorylation could reflect down-modulation through known feedback regulatory mechanisms (Haruta et al., 2000; O'Reilly et al., 2006). In this case, downstream effectors might be active even though p-AKT levels are suppressed. To test this, we examined RPPA data corresponding to the AKT substrates GSK3β and TSC2 in the NCI60 panel. Phosphorylation of both substrates was reduced in *PIK3CA*-mutant cells compared to *PTEN*-null cells (Figures 1E and 1F). Immunoblot studies confirmed a tight correlation between p-GSK3β and p-AKT (Figure S3C). Furthermore, we observed no correlation between phosphorylation or activity of p70S6 kinase (a known modulator of the feedback loop (Haruta et al., 2000; O'Reilly et al., 2006)) and p-AKT levels in *PIK3CA*-mutant cells (M.A.D. and R.R., unpublished observations). Thus, decreased p-AKT correlated with reduced substrate phosphorylation, suggesting that feedback loops do not fully explain the AKT signaling dynamics in these *PIK3CA*-mutant cells.

We also assessed functional AKT signaling by examining localization of the Forkhead transcription factor (FOXO), a direct AKT substrate, using a GFP-FOXO1 fusion construct (Brunet et al., 1999; Nakamura et al., 2000). Activated AKT phosphorylates FOXO transcription factors and prevents their nuclear entry (Brunet et al., 1999). In these experiments, GFP-FOXO1 localized to the cytoplasm in PTEN-null cells (786−0 and LNCaP; Figure 1D) and in *PIK3CA*–mutant cells with robust p-AKT expression (T47D and HCC1954; Figure 1G), consistent with downstream pathway activation (Nakamura et al., 2000). However, *PIK3CA*-mutant cells with low p-AKT (MCF-7, HCT-15, HCT-116 and SW-948) exhibited nuclear GFP-FOXO1, comparable to cells with a “wild-type” PI3K pathway (ACHN and DU-145; Figure 1G), and to the effects of a GFP-FOXO1-A3 construct resistant to AKT-mediated cytoplasmic localization (Figure S3D). Together with the RPPA and immunoblotting data, these results provided strong evidence that AKT signaling is often diminished in *PIK3CA*-mutant cancers.

PIK3CA-mutant cells with low p-AKT show reduced dependence on AKT for tumorigenicity

We next determined whether AKT-dependent signaling is required for tumorigenicity in *PIK3CA*-mutant cells. Here, we examined anchorage-independent growth on soft agar following lentiviral RNAi knockdown (Moffat et al., 2006). Since many cancer cells express multiple AKT isoforms (Figure S5A), we also tested a dominant negative AKT construct (Dudek et al., 1997), which inhibits all AKT variants (dnAKT). Suppression of *AKT1* reduced soft agar growth in PTEN-null cells (786−0) and *PIK3CA*-mutant cells with high p-AKT (T47D and HCC1954; Figures 2A and S4A). In contrast, neither *AKT1* knockdown nor dominant-negative inhibition had any discernible effect on anchorage-independent growth in *PIK3CA*–mutant cell lines with low p-AKT (MCF-7, SW948 and HCT-15; Figures 2A, 2C and S4B). Similarly, combined knockdown of *AKT1* and *AKT2* (Figure S5B) had only minimal effects on MCF-7 cell growth (*PIK3CA*-mutant, low p-AKT; Figures S5C and S5D). In contrast, combined AKT1/2 knockdown was highly deleterious to PTEN-null cells with elevated p-AKT (786−0 cells; Figure S5D and data not shown).

To confirm dependency on the PI3K pathway in *PIK3CA*-mutant cells, we performed shRNA-mediated knockdown of *PI3KCA* expression. As expected, *PIK3CA* knockdown markedly reduced the anchorage-independent growth of several exemplary *PIK3CA*-mutant cell lines, regardless of p-AKT levels (MCF-7, SW948, and T47D; Figure 2B). Interestingly, *PIK3CA* knockdown had no effect on anchorage-independent growth or p-AKT levels in 786−0 cells (PTEN-null; Figures 2B and S4C), suggesting the involvement of another PI3K isoform (e.g., p110β; Jia et al., 2008; Torbett et al., 2008)) or more than one PI3K isoform in these cells (Hooshmand-Rad et al., 2000). Together, these observations suggested that *PIK3CA*–mutant

cells with low p-AKT may exhibit a reduced dependence on AKT signaling, although these cells remain dependent on *PIK3CA* for their tumorigenicity.

AKT membrane localization correlates with 3'-phosphatidylinositol levels in *PIK3CA*-mutant cells

Next, we sought to understand the mechanism whereby AKT fails to under undergo robust activation despite the presence of oncogenic *PIK3CA* mutations. To become activated, AKT is recruited to the plasma membrane through its PH domain by PI3K-derived phosphatidylinositols. Therefore, we examined the cellular localization of AKT in PTEN-null or *PIK3CA*-mutant cells. Transient transfection of a construct expressing the AKT PH domain fused to green fluorescent protein (PH-AKT-GFP; Varnai and Balla, 1998; Watton and Downward, 1999)) under serum-starved conditions resulted in GFP membrane localization in PTEN-null cells (786−0) and *PIK3CA*–mutant cells with elevated p-AKT (HCC1954 and T47D), but not in *PIK3CA*–mutant cells with low p-AKT (MCF-7 and SW-948; Figure 3A, upper panel). Immunofluorescence studies of endogenous AKT1 yielded similar results (Figure S6A). These results suggested that the diminutive AKT signaling in some *PIK3CA*-mutant contexts may result from its inefficient translocation to the plasma membrane.

We next examined the abundance of PI3K-derived phosphatidylinositide products in relation to the mode of PI3K activation (Vanhaesebroeck et al., 2001). Using a monoclonal antibody recognizing PtdIns(3,4,5)P_3 (Figure S6B), we found that PTEN-null cells (786−0) and *PIK3CA*–mutant cells with elevated p-AKT (T47D and HCC1954) showed robust membrane staining for this phospholipid (Figure 3A, lower panel), whereas *PIK3CA*–mutant cells with low p-AKT (MCF-7 and SW-948) showed reduced PtdIns(3,4,5)P_3 (Figure 3A, lower panel). The fluorescence intensity of this antibody was suppressed following incubation with the PI3K inhibitor LY-294002 (Figure S6B), suggesting a specific recognition of PI3K-derived phosphatidylinositide products. To confirm these experiments, we measured phosphatidylinositide levels directly by ^{3}[H]-inositol-based metabolic labeling studies. Both PI(3,4,5)P_3 and PI(3,4)P_2 were significantly reduced in *PIK3CA*-mutant cell lines with low p-AKT compared to *PIK3CA*-mutant cells with high p-AKT (Figures 3B and 3C). Together, these results suggested that reduced levels of key PI3K phosphatidylinositide products may impair AKT membrane localization (and subsequent activation) in some *PIK3CA*-mutant cells.

PTEN regulates AKT activation in *PIK3CA*-mutant cells

The direct correlation between AKT phosphorylation, membrane localization, and PI3K phospholipid products also suggested that PTEN activity might suppress AKT activation in some *PIK3CA*-mutant cells by constraining phosphatidylinositide accumulation. This notion was buttressed by our observations that most *PIK3CA*-mutant cells with low p-AKT robustly expressed wild-type PTEN (Figures 1D and S2B). To test this, we performed shRNA knockdown of PTEN in PI3K pathway "wild-type" cells (DU-145) or *PIK3CA*-mutant cells with low p-AKT (MCF-7) and measured p-AKT levels. As expected, AKT phosphorylation at both Ser473 and Thr308 was induced upon PTEN knockdown (Figure 3D), suggesting that PTEN may play a dominant role in AKT regulation, even in the presence of oncogenic *PIK3CA* mutations.

PDK1 is highly expressed and required for tumorigenicity in *PIK3CA*-mutant cancer cells

The Pleckstrin-homology (PH) domain-containing kinase PDK1 is also recruited to cell membranes in response to PI3K activation, and is independently required for PI3K-mediated transformation in several systems (Bayascas et al., 2005; Flynn et al., 2000; Zeng et al., 2002). To examine PDK1 activity in relation to *PIK3CA* mutation, we performed an RPPA analysis of 224 hormone receptor (+) human breast tumor specimens using an antibody recognizing p-PDK1 at Ser241, indicative of activation (Casamayor et al., 1999). Notably,

elevated p-PDK1 levels in association with both *PI3KCA*^{helical} and *PI3KCA*^{kinase} mutations were observed in this tumor panel ($p = 0.01$ compared to "wild type" tumors for each mutation; Figure 4A), confirming robust PDK1 expression and activation in the setting of *PIK3CA* mutation in vivo. To determine if this phenomenon was manifest in vitro, we also examined activated PDK1 levels in our panel of PTEN-null or *PIK3CA*-mutant cell lines. Consistent with the breast tumor findings, all *PIK3CA*-mutant cell lines examined showed robust p-PDK1 levels, regardless of mutation type and p-AKT levels (Figures 4B and 4C), although p-PDK1 was not affected by treatment with LY-294002 (data not shown). Moreover, increased p-PDK1 was also linked significantly to *PI3KCA*^{helical} cells in a follow-up RPPA analysis of 51 breast cancer cell lines ($p = 0.03$ compared to "wild-type" cells; Figure S7B), despite the reduced p-AKT levels in this subset (Figures S1B and S1C).

We then considered whether *PIK3CA*-mutant cancer cells with low p-AKT remained dependent on PDK1 signaling. As expected, *PDK1* knockdown strongly suppressed anchorage independent growth in representative *PIK3CA*^{helical} (MCF-7), *PIK3CA*^{kinase} (T47D), and PTEN-null cells (786−0) (Figures 4D, 4E and S7C), indicating a functional dependence on PDK1 in these cells. Thus, activated PDK1 is highly expressed and required for tumorigenicity in cancers harboring *PIK3CA* mutations.

PDK1 shows PI3K-dependent membrane localization in *PIK3CA*-mutant cells

To study PDK1 activation in more detail, we performed immunofluorescence studies under serum-starved conditions following transfection of a construct expressing the PH domain of PDK1 fused to GFP (PH-PDK1-GFP). In contrast to the analogous experiments with PH-AKT-GFP above, PH-PDK1-GFP fluorescence accumulated at the plasma membrane in all PTEN-null and *PIK3CA*-mutant cell lines examined, regardless of p-AKT levels; but this membrane localization was less evident in PI3K pathway "wild-type" cells (Figure 5A). Moreover, membrane GFP fluorescence was reduced following treatment with LY-294002, suggesting that PH-PDK1 membrane localization was PI3 kinase-dependent (Figure 5A). These results indicated that PI3 kinase-driven PDK1 signaling remained robust even when AKT-dependent signaling was reduced.

We also studied PDK1 membrane localization by a more sensitive approach involving separation of membrane and cytosolic fractions under serum-starved conditions. Endogenous p-AKT, total AKT, p-PDK1 (Ser241) and total PDK1 were measured in each fraction. In PTEN-null cells (786−0) and *PIK3CA*–mutant cells with high p-AKT (HCC1954), both p-AKT and p-PDK1 were present in the membrane fractions (Figure 5B). Membrane p-PDK1 and total PDK1 were also detectable in *PIK3CA*–mutant cells with low p-AKT (MCF-7, HCT15, and SW-948); however, membrane p-AKT was not identified (Figures 5B and S7D). We then examined PDK1 localization following lentiviral RNAi knockdown of *PIK3CA*. Reduction of *PIK3CA* expression by two independent shRNAs resulted in a measurable decrease in membrane PDK1 in MCF-7 cells under serum-starved conditions (Figures 5C and 5D). These results lent additional credence to the notion that oncogenic p110α localization in *PIK3CA*-mutant cancer cells, even when AKT signaling is diminished.

SGK3 is required for AKT-independent viability in *PIK3CA*-mutant cancer cells

Next, we investigated possible mechanisms of PDK1-dependent, AKT-independent growth in *PIK3CA*-mutant cells. Here, we screened 6 *PIK3CA*-mutant human cancer cell lines (Table S1) using a lentiviral shRNA library targeting >1000 kinases, phosphatases, and other cancer genes (Boehm et al., 2007;Moffat et al., 2006), including 20 known PDK1 substrates (Table S2). We stratified the *PIK3CA*-mutant lines into two groups based on p-AKT levels (3 lines with elevated p-AKT and 3 with low p-AKT) and analyzed the top 10% of 120 shRNAs targeting PDK1 substrates whose effects on viability distinguished these two classes (illustrated

schematically in Figure S8A). We considered a gene a "hit" if two or more shRNAs against this gene suppressed viability with a B-score < −1 (Experimental Procedures).

Interestingly, only 1 of 20 PDK1 substrates met the aforementioned criteria in each *PIK3CA*-mutant class. *AKT1* knockdown most strongly suppressed viability in *PIK3CA*-mutant cells with high p-AKT, as expected (Figures 6A and 6B). Multiple *AKT2* hairpins also segregated within the top 10% of hairpins distinguishing the high p-AKT class (Supplemental Figure 8A), though their absolute effects on cell viability were more modest, consistent with lower abundance of this AKT isoform in many cell types. The knockdown efficacy of multiple shAKT1 hairpins was confirmed by RT-PCR analysis and immunoblotting (Figure S8B). In contrast, hairpins targeting *SGK3* (serum/glucocorticoid regulated kinase 3; also known as *CISK*) most strongly suppressed viability in "low p-AKT" *PIK3CA*-mutant cells (Figures 6A and 6C). SGK3 is an intriguing candidate PDK1 effector; this kinase shares ~50% identity with AKT and contains a PX domain, which binds phosphatidylinositols (Tessier and Woodgett, 2006). We confirmed knockdown efficacy of the two most potent shSGK3 hairpins by RT-PCR (Figure S8C) and immunoblotting (Figure 6D). SGK3 knockdown strongly suppressed MCF-7 cell viability (Figure 6D), in marked contrast to the effects of AKT knockdown (Figures 2A, 2C, and S5B-D). Thus, multiple *PIK3CA*–mutant cells that lacked AKT activation showed a functional dependency on SGK3.

SGK3 is regulated by PDK1 and PI3K in *PIK3CA*-mutant cancer cells with low p-AKT

To confirm PDK1-dependent modulation of SGK3 and other known PDK1 substrates in *PIK3CA*-mutant cells, we suppressed PDK1 expression and examined the resulting phosphorylation patterns (Vanhaesebroeck and Alessi, 2000). PDK1 knockdown substantially diminished phosphorylation of SGK3 at Thr320 in MCF-7 cells (low p-AKT), but this effect was less apparent in T47D cells (elevated p-AKT) (Figure 7A). In contrast, protein kinase C beta/zeta phosphorylation was only minimally suppressed in MCF-7 and not at all in T47D (Figure 7A). PDK1 knockdown also reduced p-p70S6K(Thr229) and p-RSK(Ser227) in both cell lines; however, these PDK1 substrates were not identified as selective dependencies in our RNAi analysis. As expected, PDK1 knockdown suppressed p-AKT (Thr308) in T47D cells (Figure 7A). Overall, these results provide biochemical evidence that SGK3 contributes to an AKT-independent signal downstream of PDK1 in *PIK3CA*-mutant cells, although the importance of additional PDK1 substrates and alternate effectors cannot be excluded.

We then tested whether SGK3 activity is regulated by PI3K in the *PIK3CA*-mutant context. The PX domain confers endosomal localization of SGK3 through its avidity for phosphatidylinositide-3-phosphate, which is present at high levels on endosomal membranes. As expected, a construct expressing the SGK3 PX domain fused to GFP localized to endosomes in all cancer cell lines examined (Figure S9A); this localization was unaffected by treatment with LY-294002 (Figure S9A). However, LY-294002 markedly reduced PDK1-dependent SGK3(T320) phosphorylation (Figures S9B-C) in *PIK3CA*-mutant cells with low p-AKT (MCF-7 and HCT-15 cells; Figure 7B). Thus, SGK3 activation but not endosomal localization is regulated by PI3K in the setting of *PIK3CA* mutation.

Next, we determined the extent to which SGK3 exhibits PDK1-dependent phosphorylation in cancer cells and its relation to *PTEN* or *PIK3CA* mutation. Although p-SGK3(T320) was undetectable in non-transformed cells (MCF-10A and MCF-12A cells; Figure 7C). This phosphorylation event was evident in multiple cancer cell lines, including most *PIK3CA*-mutant cells examined (Figure 7C). Furthermore, only SGK3, and not SGK1 or SGK2, was consistently expressed across all relevant *PIK3CA*-mutant cell lines in our panel (Figure S9D). Taken together, these results suggest that SGK3 activation may be a characteristic of many cancers independent of AKT signaling.

Discussion

Aberrant PI3K signaling has been studied extensively in cancer. This study provides evidence that *PIK3CA* mutations may contribute to tumorigenicity through both AKT-dependent and AKT-independent mechanisms. In the absence of AKT activation, PDK1 may transmit an alternative signal that engages alternative downstream substrates such as SGK3 in *PIK3CA*-mutant cancer cells. This study thereby nominates both PDK1 and SGK3 as key oncogenic effectors downstream of activating *PIK3CA* mutations.

Our AKT signaling results differ from studies in which mutant *PIK3CA* was expressed ectopically in cell culture/chick embryo models (Isakoff et al., 2005; Kang et al., 2005; Zhao et al., 2005) or introduced by knock-in methods into immortalized breast epithelial cells (Gustin et al., 2009). On the other hand, multiple experimental lines of evidence presented herein suggest that steady-state AKT signaling is reduced in many malignant contexts where *PIK3CA*-mutations are present in situ. Moreover, the AKT and PDK1 activation patterns that we observe are consistent across many human cell lines and clinical breast tumor specimens, in line with published observations (Stemke-Hale et al., 2008). Of course, we cannot completely exclude the possibility that AKT signaling operates at very low levels in some *PIK3CA*-mutant cancers, even when poorly detectable by conventional methods. However, our findings suggest that in some settings the functional “output” of *PIK3CA* mutations differs importantly from that of deregulated PI3 kinase activity observed in PTEN-null cells.

Studies that employ selective small molecule AKT inhibitors may help clarify the nature of AKT dependency in *PIK3CA*-mutant cancers. Consistent with our results, sensitivity in vitro to inhibition by small molecule allosteric AKT1/2 inhibitors has been correlated strongly with AKT phosphorylation in human cancer cell lines (She et al., 2008). In the study by She et al., (2008), p-AKT was detectable in MCF7 cells and suppressed by an AKT inhibitor. Nonetheless, MCF-7 cells exhibited an attenuated sensitivity to pharmacologic AKT1/2 inhibition compared to several cancer cell lines with markedly elevated p-AKT levels (EC50 ~1 uM; She et al., 2008). In our hands, AKT phosphorylation occasionally becomes detectable in MCF-7 cells after prolonged cultivation *in vitro* (e.g., ~1 year; K.M.V., unpublished observations), suggesting that variances in cell culture conditions may influence p-AKT levels in some cases. Other studies have found *PIK3CA*-mutant breast cancer cell lines to be generally more sensitive than *PIK3CA*-mutant colon cancer cell lines to small molecule AKT inhibition, suggesting that cell lineage effects may also modulate this pharmacologic sensitivity (Greshock, 2008). Altogether, these results endorse the notion that high p-AKT levels denote an AKT dependency in *PIK3CA*-mutant cancer cells, while allowing for the possibility of AKT-independent signaling in settings where steady-state p-AKT is reduced.

Both “upstream” activation (through receptor tyrosine kinases, RAS signaling, or deficiencies in feedback regulation) and PTEN function provide important modes of PI3K regulation in cancer. Interestingly, several *PIK3CA*–mutant breast cancer cell lines with high p-AKT examined herein have been shown previously to harbor either *ERBB2* overexpression/amplification (MDA-MB-453 and HCC-1954) (Blend et al., 2003; Miller et al., 1996) or high levels of activated EGFR (BT-20) (Zhang et al., 2002). Also, *PIK3CA*-mutant cells and human breast tumors with low p-AKT tend to express wild-type PTEN and reduced 3’-phoshpatidylinositides, whereas PTEN knockdown results in robust AKT phosphorylation. Thus, many *PIK3CA*-mutant cancers that depend on AKT signaling may contain concomitant upstream signal deregulation (e.g., RTK/RAS activation or loss of feedback regulation) or PTEN deficiency (Oda et al., 2005). However, *PIK3CA* mutation by itself is neither necessary nor sufficient for full AKT pathway activation when it occurs *in situ.*

PIK3CA-mutant cells exhibit robust p-PDK1 expression and membrane recruitment, regardless of AKT signaling. PDK1 exists in a constitutively active conformation that is not known to be further augmented by upstream signals (Casamayor et al., 1999). Oncogenic membrane recruitment of PDK1 appears to depend at least partially on mutant *PIK3CA* (Figures 5A-D). Differential membrane localization of PDK1 compared to AKT may relate in part to differing PH-domain phosphatidylinositide binding affinities, since prior studies suggest that PDK1 may exhibit ~20 fold higher affinity for $PI(3,4,5)P_3$ than AKT (Stephens et al., 1998; (Currie et al., 1999). PDK1 recruitment might also be aided by a kinase-independent function of mutant *PIK3CA*, such as stabilization of a RTK-adapter protein complex that permits phosphatidylinositol-independent PDK1 membrane localization. Towards this end, PDK1 was shown to bind the Grb14 adapter protein in a PH-domain independent fashion (King and Newton, 2004). Thus, while AKT membrane localization (and subsequent activation) depends critically on elevated $PI(3,4)P_2$ and $PI(3,4,5)P_3$ levels, PDK1 localization may require a lesser degree of phosphatidylinositide accumulation.

PIK3CA-mutant cancer cells with low AKT signaling exhibit a selective dependency on SGK3 for viability. The SGK family of AGC kinases shares more than 50% identity with the AKT kinase domain (Tessier and Woodgett, 2006). SGK proteins become direct PDK1 substrates as a result of C-terminal hydrophobic motif (HM) phosphorylation (Frodin et al., 2002; Sarbassov et al., 2005). Recent evidence suggests that HM phosphorylation within SGK is mediated by the TORC2 complex (Garcia-Martinez and Alessi, 2008), and that SGK proteins may function as critical mediators of cell growth downstream of rictor/TORC2 (Jones et al., 2009; Soukas et al., 2009). In accordance with previous findings, here we show that PDK1-dependent SGK3 activation is under PI3K regulation in *PIK3CA*-mutant cancer cells. The SGK3 PX domain exhibits a particular affinity for phosphatidylinositol 3' phosphate (Tessier and Woodgett, 2006), which localizes SGK3 to endosomal membranes (Figure S9A) (Virbasius et al., 2001). SGK3 recruits PDK1 to endosomes upon PI-3 kinase activation (Slagsvold et al., 2006). These phenomena raise the intriguing possibility that mutant p110α may convey its oncogenic signal from or within endosomal compartments.

The precise oncogenic signal elaborated by SGK3 remains obscure, as few endosomal SGK3 substrates have been identified. The E3 ubiquitin ligase AIP4 was identified as an endosomal SGK3 substrate whose phosphorylation leads to stabilization of CXCR4 and promotes breast cancer metastasis (Slagsvold et al., 2006). The mammalian homologue of Drosophila Flightless I (FLI-I) is another putative SGK3 substrate (Xu et al., 2009). FLI-I phosphorylation may protect hematopoietic cells from death induced by cytokine withdrawal. Additional studies should inform whether AIP4 or FLI-I confer tumorigenic signals relevant to the *PIK3CA*-mutant context.

Together, our observations offer a modified conceptual framework for oncogenic PI3K signaling. In the setting of PTEN deficiency, excess upstream activation, or defective feedback regulation, *PIK3CA*-mutant cancers may elaborate sufficient membrane 3'-phosphatidylinositols to recruit both AKT and PDK1 to the plasma membrane. When this occurs, tumors will exhibit a robust (and usually "addictive") AKT-dependent signal. On the other hand, if PTEN function remains intact and upstream or feedback pathways are not fully dysregulated, *PIK3CA*-mutations may transduce an AKT-independent signal that engages PDK1 and SGK3. Unlike AKT activation, which requires simultaneous and sufficient membrane recruitment of multiple proteins following 3'-phosphatidylinositol synthesis, a moderate degree of PDK1 (endosomal) membrane localization may be all that is required to activate SGK3 in a PI3K-dependent manner.

In summary, this study has uncovered an AKT-independent signal transmitted downstream of many *PIK3CA*-mutant cancers. These results provide a mechanistic basis for recent

observations suggesting biological differences between *PIK3CA* and PTEN mutation in human tumors (Saal et al., 2007; Stemke-Hale et al., 2008). Moreover, they suggest that inhibition of PI3K, PDK1 and downstream effectors may in some cases be more effective than inhibition of AKT. Several PI3K pathway inhibitors have entered clinical trials. Knowledge of the differential signaling pathways could thus inform the design of clinical trials in cancers defined by PI3K pathway mutations.

Experimental Procedures

Lentiviral shRNAs and Plasmids

All lentiviral shRNA constructs were constructed in the pLKO.1puro vector (http://www.broad.mit.edu/genome_bio/trc). A list of lentiviral shRNAs used is shown in Table S3. The GFP-FOXO fusion construct was described previously (Nakamura et al., 2000). The plasmid pcDNA3-PH-AKT-GFP (Varnai and Balla, 1998) was a kind gift from Dr. Tamas Balla, National Institute of Health (Bethesda, MD).

Cell Culture

NCI60 cell lines were kindly provided by S. Holbeck of the Developmental Therapeutics Program of the National Cancer Institute. NCI60 cell lines were grown in RPMI 1640 medium containing 5% fetal bovine serum and 2 mM L-glutamine, and harvested at 50−80% confluence. Protein lysates were prepared from 51 human breast cancer cell lines using standard methods (see RPPA section below), and were provided by Dr. Joe Gray, Lawrence Berkeley National Laboratories (Berkeley, CA). 786−0, LNCaP, MDA-MB-361, SW-948, BT-20, HCC1954, T47D, MDA-MB-453, SK-OV3, HCT-15, DU145, ACHN and MCF-7 cells were purchased from the American Type Culture Collection (Manassas, VA), and cultured in media according to the suppliers' instructions. MCF-10A and MCF12A cells were provided by Dr. Kornelia Polyak at Dana-Farber Cancer Institute, Boston. *PIK3CA* exons 9 and 20 were resequenced in all $PIK3CA^{helical}$ and $PIK3CA^{kinase}$ cells to confirm the presence of the relevant mutations.

Breast Tumor Specimens

For the analysis of p-AKT and PTEN levels *in vivo*, 64 hormone receptor-positive breast tumor samples were obtained from patients with stages I-III adenocarcinoma and frozen in the Breast Tumor Tissue Bank at the M.D. Anderson Cancer Center (MDACC). For the subsequent studies of p-PDK1, an additional 160 tumors were analyzed from specimens that were obtained from the Breast Tissue Frozen Tumor Bank at MDACC (A.S.) and from Clinic Hospital (CH), Valencia, Spain (A.L.H.). All specimens were collected and studied under IRB-approved protocols at MDACC and CH through which informed consent was obtained or de-identified specimens were used. Pathologic assessment confirmed that each sample used was composed of at least 70% tumor cells. Tumors were lysed and protein extracted for RPPA as described below. DNA was extracted from the tumors and used for *PIK3CA* mutation detection or *PTEN* sequencing as described below.

Reverse Phase Protein Lysate Array (RPPA) analysis

RPPA assays were performed as described previously (Tibes et al., 2006) in Supplemental Experimental Procedures. Unsupervised hierarchical clustering was performed on mean-centered protein expression values using Cluster 2.1 software (http://rana.lbl.gov/EisenSoftware.htm). Results were visualized using Treeview software (http://rana.lbl.gov/EisenSoftware.htm). Correlations between protein levels were calculated using Microsoft Excel (Seattle, WA). Significance of these correlations was determined by canonical correlations using NCSS Statistical and Power Analysis software (Kaysville, UT).

Differences between groups were assessed and visualized using MATLAB software (Natick, MA).

Immunoblot Analysis, Transfections and Fluorescence Microscopy

Antibodies recognizing total AKT, AKT1, phospho-AKT (S473 and T308), AKT2, AKT3, PTEN, p110α, phospho-PDK1 (S241), Pan-Cadherin, GAPDH, GSK3β phospho-GSK3β (Ser-9), phospho-SGK3 (T320 – special order) were obtained from Cell Signaling Technology. Antibody recognizing PDK1 was obtained from BD Biosciences. Phospho-PKC-zeta (T410), PKC-zeta, RSK2, p70-S6 kinase antibodies were obtained from Santa Cruz Biotechnology. Phospho-RSK (T227) and phospho-p70-S6 kinase antibodies were purchased from R&D Biosystems. SGK3 antibody was purchased from AbD Serotec. SGK1, SGK2 and β-actin antibodies were obtained from Sigma. Methodological details are provided in Supplemental Experimental Procedures.

Virus Production, Titration and Infection

Lentiviruses were produced by transfection of 293ε cells with the packaging plasmids encoding Δ8.9 and VSV-G along with the lentiviral shRNA vector using Lipofectamine 2000 reagent, according to the manufacturer's instructions. To perform lentiviral infections, the target cells were plated at 40−50% confluence and incubated overnight (16 hr). On the day of infections, the culture medium was replaced by the appropriately titered viral supernatant (1.5 ml/well) and incubated at 37° C for 10 hours; afterwards, the viral supernatant was replaced with fresh media. Forty-eight hours later, infected cell populations were selected in puromycin (2μg/ml): After 5 days of selection, shRNA knockdown efficiency was determined by Western blot analysis for respective proteins using specific antibodies.

Anchorage Independent Growth Assays

Methods are described in Supplemental Experimental Procedures.

Cell Proliferation Assay

Methods are described in Supplemental Experimental Procedures.

^{3}H Lipid Labeling Experiments

Cells were labeled with [^{3}H]-inositol for 72 hours in inositol-free and serum-free medium. After labeling, cells were lysed in 1 M HCl. Lipids were extracted using chloroform/methanol (1:1, vol/vol) and deacylated as described (Serunian et al., 1991). Briefly, deacylated lipids were separated by anionic-exchange HPLC, detected by an online radiomatic detector, and quantified by using the FLO-ONE analysis program (Packard). Each peak was identified by using *in vitro*-synthesized internal standard lipids. The counts present in each peak were normalized against the counts present in the phosphatidylinositol peak. *p* values were determined using a one-tailed Student's t-test of the means of three *PIK3CA*-mutant cell lines with low p-AKT (MCF-7, HCT-15, and SW-948) and three with high p-AKT (T-47D, HCC1954, and MDA-MB453).

RNAi screen

Lentiviral shRNA infections were performed as described previously (Boehm et al., 2007; Moffat et al., 2006). Briefly, lentiviral infections were performed in high throughput using a subset of the TRC library containing approximately 5000 shRNA directed primarily against kinases and phosphatases(Boehm et al., 2007); data from known PDK1 substrates was extracted from this screen. On average, five unique shRNA were tested per gene for redundant coverage. Updated protocols for high throughput viral production and infection, as well as a

database of hairpin designs are available online at http://www.broad.mit.edu/genome_bio/trc/rnai.html. Target cells were infected in 384 well plates in quadruplicate, with two “puromycin-plus” and two “puromycin-minus” replicates to assess for infection efficiency. Cell Titer Glo (Promega) was used to measure viability on average 6 days following lentiviral infection for most cell lines.

Data for each shRNA was normalized using the B-score, an analog of the Z-score that uses a two-way median polish to minimize row/column effects, and normalization to the median absolute deviation to account for plate-to-plate (Malo et al., 2006). shRNA B-score data was analyzed using the Comparative Marker Selection application suite in GenePattern(Gould et al., 2006). Distinguishing hairpins were ranked using either the t-test statistic or the signal to noise ratio (SNR), measures of the difference in class mean viability scores and the standard deviation across samples. Individual shRNA B-score data for each cell line was aligned and assembled into a .res file as an input into the Comparative Marker Selection application. Standard classification files were used to generate each of the class distinctions. shRNA viability data was ranked according to the t-test statistic, and the top 10% shRNAs distinguishing the class of interest were filtered for genes with multiple hairpins to minimize potential off-target effects. In addition, at least one shRNA was required to promote significant viability loss across the class (mean B-score <-1), and one shRNA was required to yield a false discovery rate (FDR) <25% for the comparison.

Supplementary Material

Refer to Web version on PubMed Central for supplementary material.

Acknowledgements

We thank Erica Bauerlein for shRNA constructs, Len Pennacchio, Jan-Fang Cheng, Mandy Madiredio, Stefan Frohling, Claudia Scholl, and Raymond Wadlow for technical assistance; Tamas Balla for the PH-AKT GFP construct; Pablo Tamayo for statistical help; and Payman Amiri, Stephen Basham, Amit Dutt, Matthew Meyerson, David Livingston, David Sabatini, and members of the Garraway lab for helpful discussions. This work was supported by the Prostate Cancer Foundation, the Burroughs-Wellcome Fund (LAG), the Department of Defense grant PC073284 (KMV), the American Society for Clinical Oncology (MAD), Human Frontier Fellowship Organization (JHR), National Human Genome Research Institute (ESL), the Susan Madden Fund (DAB), Starr Cancer Consortium 1A-11 (WCH), and the National Institutes of Health under grants T32CA09172-33 (DAB), P50CA093459 (MAD), R33CA128625, P01CA050661 (WCH), P50CA112967, P30CA14051 (TJ), R01CA085912 (WRS, LAG) and DP2OD002750-01 (LAG).

References

Alessi DR, James SR, Downes CP, Holmes AB, Gaffney PR, Reese CB, Cohen P. Characterization of a 3-phosphoinositide-dependent protein kinase which phosphorylates and activates protein kinase Balpha. Curr Biol 1997;7:261–269. [PubMed: 9094314]

Barbareschi M, Buttitta F, Felicioni L, Cotrupi S, Barassi F, Del Grammastro M, Ferro A, Dalla Palma P, Galligioni E, Marchetti A. Different prognostic roles of mutations in the helical and kinase domains of the PIK3CA gene in breast carcinomas. Clin Cancer Res 2007;13:6064–6069. [PubMed: 17947469]

Bayascas JR, Leslie NR, Parsons R, Fleming S, Alessi DR. Hypomorphic mutation of PDK1 suppresses tumorigenesis in PTEN(+/−) mice. Curr Biol 2005;15:1839–1846. [PubMed: 16243031]

Blend MJ, Stastny JJ, Swanson SM, Brechbiel MW. Labeling anti-HER2/neu monoclonal antibodies with 111In and 90Y using a bifunctional DTPA chelating agent. Cancer Biother Radiopharm 2003;18:355–363. [PubMed: 12954122]

Boehm JS, Zhao JJ, Yao J, Kim SY, Firestein R, Dunn IF, Sjostrom SK, Garraway LA, Weremowicz S, Richardson AL, et al. Integrative genomic approaches identify IKBKE as a breast cancer oncogene. Cell 2007;129:1065–1079. [PubMed: 17574021]

Brunet A, Bonni A, Zigmond MJ, Lin MZ, Juo P, Hu LS, Anderson MJ, Arden KC, Blenis J, Greenberg ME. Akt promotes cell survival by phosphorylating and inhibiting a Forkhead transcription factor. Cell 1999;96:857–868. [PubMed: 10102273]

Carpten JD, Faber AL, Horn C, Donoho GP, Briggs SL, Robbins CM, Hostetter G, Boguslawski S, Moses TY, Savage S, et al. A transforming mutation in the pleckstrin homology domain of AKT1 in cancer. Nature 2007;448:439–444. [PubMed: 17611497]

Casamayor A, Morrice NA, Alessi DR. Phosphorylation of Ser-241 is essential for the activity of 3-phosphoinositide-dependent protein kinase-1: identification of five sites of phosphorylation in vivo. The Biochemical journal 1999;342(Pt 2):287–292. [PubMed: 10455013]

Currie RA, Walker KS, Gray A, Deak M, Casamayor A, Downes CP, Cohen P, Alessi DR, Lucocq J. Role of phosphatidylinositol 3,4,5-trisphosphate in regulating the activity and localization of 3-phosphoinositide-dependent protein kinase-1. The Biochemical journal 1999;337(Pt 3):575–583. [PubMed: 9895304]

Depowski PL, Rosenthal SI, Ross JS. Loss of expression of the PTEN gene protein product is associated with poor outcome in breast cancer. Mod Pathol 2001;14:672–676. [PubMed: 11454999]

Dudek H, Datta SR, Franke TF, Birnbaum MJ, Yao R, Cooper GM, Segal RA, Kaplan DR, Greenberg ME. Regulation of neuronal survival by the serinethreonine protein kinase Akt. Science (New York, NY 1997;275:661–665.

Engelman JA, Luo J, Cantley LC. The evolution of phosphatidylinositol 3-kinases as regulators of growth and metabolism. Nat Rev Genet 2006;7:606–619. [PubMed: 16847462]

Flynn P, Wongdagger M, Zavar M, Dean NM, Stokoe D. Inhibition of PDK-1 activity causes a reduction in cell proliferation and survival. Curr Biol 2000;10:1439–1442. [PubMed: 11102805]

Frodin M, Antal TL, Dummler BA, Jensen CJ, Deak M, Gammeltoft S, Biondi RM. A phosphoserine/threonine-binding pocket in AGC kinases and PDK1 mediates activation by hydrophobic motif phosphorylation. The EMBO journal 2002;21:5396–5407. [PubMed: 12374740]

Garcia-Martinez JM, Alessi DR. mTOR complex 2 (mTORC2) controls hydrophobic motif phosphorylation and activation of serum- and glucocorticoid-induced protein kinase 1 (SGK1). The Biochemical journal 2008;416:375–385. [PubMed: 18925875]

Gould J, Getz G, Monti S, Reich M, Mesirov JP. Comparative gene marker selection suite. Bioinformatics 2006;22:1924–1925. [PubMed: 16709585]

Greshock, J. In American Association for Cancer Research: Targeting the PI3-Kinase Pathway in Cancer. Cambridge, MA: 2008. In vitro Sensitivity Data Identifies Tumor Types and Molecular Subtypes that Predict Response to the PI3-kinase Inhibitor GSK1059615 and the AKT Inhibitor GSK690693..

Gustin JP, Karakas B, Weiss MB, Abukhdeir AM, Lauring J, Garay JP, Cosgrove D, Tamaki A, Konishi H, Konishi Y, et al. Knockin of mutant PIK3CA activates multiple oncogenic pathways. Proceedings of the National Academy of Sciences of the United States of America 2009;106:2835–2840. [PubMed: 19196980]

Haruta T, Uno T, Kawahara J, Takano A, Egawa K, Sharma PM, Olefsky JM, Kobayashi M. A rapamycin-sensitive pathway down-regulates insulin signaling via phosphorylation and proteasomal degradation of insulin receptor substrate-1. Mol Endocrinol 2000;14:783–794. [PubMed: 10847581]

Hooshmand-Rad R, Hajkova L, Klint P, Karlsson R, Vanhaesebroeck B, Claesson-Welsh L, Heldin CH. The PI 3-kinase isoforms p110(alpha) and p110(beta) have differential roles in PDGF- and insulin-mediated signaling. J Cell Sci 2000;113(Pt 2):207–214. [PubMed: 10633072]

Isakoff SJ, Engelman JA, Irie HY, Luo J, Brachmann SM, Pearline RV, Cantley LC, Brugge JS. Breast cancer-associated PIK3CA mutations are oncogenic in mammary epithelial cells. Cancer research 2005;65:10992–11000. [PubMed: 16322248]

Jia S, Liu Z, Zhang S, Liu P, Zhang L, Lee SH, Zhang J, Signoretti S, Loda M, Roberts TM, Zhao JJ. Essential roles of PI(3)K-p110 beta in cell growth, metabolism and tumorigenesis. Nature. 2008online ahead of print

Jones KT, Greer ER, Pearce D, Ashrafi K. Rictor/TORC2 Regulates Caenorhabditis elegans Fat Storage, Body Size, and Development through sgk-1. PLoS biology 2009;7:e60. [PubMed: 19260765]

Kang S, Bader AG, Vogt PK. Phosphatidylinositol 3-kinase mutations identified in human cancer are oncogenic. Proceedings of the National Academy of Sciences of the United States of America 2005;102:802–807. [PubMed: 15647370]

King CC, Newton AC. The adaptor protein Grb14 regulates the localization of 3-phosphoinositide-dependent kinase-1. The Journal of biological chemistry 2004;279:37518–37527. [PubMed: 15210700]

Lee JC, Vivanco I, Beroukhim R, Huang JH, Feng WL, DeBiasi RM, Yoshimoto K, King JC, Nghiemphu P, Yuza Y, et al. Epidermal growth factor receptor activation in glioblastoma through novel missense mutations in the extracellular domain. PLoS Med 2006;3:e485. [PubMed: 17177598]

Malo N, Hanley JA, Cerquozzi S, Pelletier J, Nadon R. Statistical practice in high-throughput screening data analysis. Nat Biotechnol 2006;24:167–175. [PubMed: 16465162]

Miller SJ, Xing X, Xi L, Hung MC. Identification of a specific DNA region required for enhanced transcription of HER2/neu in the MDA-MB453 breast cancer cell line. DNA Cell Biol 1996;15:749–757. [PubMed: 8836033]

Moffat J, Grueneberg DA, Yang X, Kim SY, Kloepfer AM, Hinkle G, Piqani B, Eisenhaure TM, Luo B, Grenier JK, et al. A lentiviral RNAi library for human and mouse genes applied to an arrayed viral high-content screen. Cell 2006;124:1283–1298. [PubMed: 16564017]

Nakamura N, Ramaswamy S, Vazquez F, Signoretti S, Loda M, Sellers WR. Forkhead transcription factors are critical effectors of cell death and cell cycle arrest downstream of PTEN. Mol Cell Biol 2000;20:8969–8982. [PubMed: 11073996]

Neve RM, Chin K, Fridlyand J, Yeh J, Baehner FL, Fevr T, Clark L, Bayani N, Coppe JP, Tong F, et al. A collection of breast cancer cell lines for the study of functionally distinct cancer subtypes. Cancer Cell 2006;10:515–527. [PubMed: 17157791]

O'Reilly KE, Rojo F, She QB, Solit D, Mills GB, Smith D, Lane H, Hofmann F, Hicklin DJ, Ludwig DL, et al. mTOR inhibition induces upstream receptor tyrosine kinase signaling and activates Akt. Cancer research 2006;66:1500–1508. [PubMed: 16452206]

Oda K, Stokoe D, Taketani Y, McCormick F. High frequency of coexistent mutations of PIK3CA and PTEN genes in endometrial carcinoma. Cancer research 2005;65:10669–10673. [PubMed: 16322209]

Saal LH, Johansson P, Holm K, Gruvberger-Saal SK, She QB, Maurer M, Koujak S, Ferrando AA, Malmstrom P, Memeo L, et al. Poor prognosis in carcinoma is associated with a gene expression signature of aberrant PTEN tumor suppressor pathway activity. Proceedings of the National Academy of Sciences of the United States of America 2007;104:7564–7569. [PubMed: 17452630]

Samuels Y, Diaz LA Jr. Schmidt-Kittler O, Cummins JM, Delong L, Cheong I, Rago C, Huso DL, Lengauer C, Kinzler KW, et al. Mutant PIK3CA promotes cell growth and invasion of human cancer cells. Cancer Cell 2005;7:561–573. [PubMed: 15950905]

Samuels Y, Wang Z, Bardelli A, Silliman N, Ptak J, Szabo S, Yan H, Gazdar A, Powell SM, Riggins GJ, et al. High frequency of mutations of the PIK3CA gene in human cancers. Science (New York, NY 2004;304:554.

Sarbassov DD, Guertin DA, Ali SM, Sabatini DM. Phosphorylation and regulation of Akt/PKB by the rictor-mTOR complex. Science (New York, NY 2005;307:1098–1101.

Serunian LA, Auger KR, Cantley LC. Identification and quantification of polyphosphoinositides produced in response to platelet-derived growth factor stimulation. Methods Enzymol 1991;198:78–87. [PubMed: 1649958]

She QB, Chandarlapaty S, Ye Q, Lobo J, Haskell KM, Leander KR, DeFeo-Jones D, Huber HE, Rosen N. Breast tumor cells with PI3K mutation or HER2 amplification are selectively addicted to Akt signaling. PLoS ONE 2008;3:e3065. [PubMed: 18725974]

Slagsvold T, Marchese A, Brech A, Stenmark H. CISK attenuates degradation of the chemokine receptor CXCR4 via the ubiquitin ligase AIP4. The EMBO journal 2006;25:3738–3749. [PubMed: 16888620]

Solit DB, Garraway LA, Pratilas CA, Sawai A, Getz G, Basso A, Ye Q, Lobo JM, She Y, Osman I, et al. BRAF mutation predicts sensitivity to MEK inhibition. Nature 2006;439:358–362. [PubMed: 16273091]

Soukas AA, Kane EA, Carr CE, Melo JA, Ruvkun G. Rictor/TORC2 regulates fat metabolism, feeding, growth, and life span in Caenorhabditis elegans. Genes & development 2009;23:496–511. [PubMed: 19240135]

Stemke-Hale K, Gonzalez-Angulo A, Lluch A, Neve RM, Davies MA, Carey M, Sahin A, Symmans WF, Pusztai L, Nolden LK, et al. An integrative genomic and proteomic analysis of PIK3CA, PTEN and AKT mutations in breast cancer. Cancer research 2008;68:6084–91. [PubMed: 18676830]

Stephens L, Anderson K, Stokoe D, Erdjument-Bromage H, Painter GF, Holmes AB, Gaffney PR, Reese CB, McCormick F, Tempst P, et al. Protein kinase B kinases that mediate phosphatidylinositol 3,4,5-trisphosphate-dependent activation of protein kinase B. Science (New York, NY 1998;279:710–714.

Stinson SF, Alley MC, Kopp WC, Fiebig HH, Mullendore LA, Pittman AF, Kenney S, Keller J, Boyd MR. Morphological and immunocytochemical characteristics of human tumor cell lines for use in a disease-oriented anticancer drug screen. Anticancer Res 1992;12:1035–1053. [PubMed: 1503399]

Tessier M, Woodgett JR. Role of the Phox homology domain and phosphorylation in activation of serum and glucocorticoid-regulated kinase-3. The Journal of biological chemistry 2006;281:23978–23989. [PubMed: 16790420]

Tibes R, Qiu Y, Lu Y, Hennessy B, Andreeff M, Mills GB, Kornblau SM. Reverse phase protein array: validation of a novel proteomic technology and utility for analysis of primary leukemia specimens and hematopoietic stem cells. Mol Cancer Ther 2006;5:2512–2521. [PubMed: 17041095]

Torbett NE, Luna A, Knight ZA, Houk A, Moasser M, Weiss W, Shokat KM, Stokoe D. A chemical screen in diverse breast cancer cell lines reveals genetic enhancers and suppressors of sensitivity to PI3K isotype-selective inhibition. The Biochemical journal. 2008

Vanhaesebroeck B, Alessi DR. The PI3K-PDK1 connection: more than just a road to PKB. The Biochemical journal 2000;346(Pt 3):561–576. [PubMed: 10698680]

Vanhaesebroeck B, Leevers SJ, Ahmadi K, Timms J, Katso R, Driscoll PC, Woscholski R, Parker PJ, Waterfield MD. Synthesis and function of 3-phosphorylated inositol lipids. Annu Rev Biochem 2001;70:535–602. [PubMed: 11395417]

Varnai P, Balla T. Visualization of phosphoinositides that bind pleckstrin homology domains: calcium- and agonist-induced dynamic changes and relationship to myo-[3H]inositol-labeled phosphoinositide pools. J Cell Biol 1998;143:501–510. [PubMed: 9786958]

Virbasius JV, Song X, Pomerleau DP, Zhan Y, Zhou GW, Czech MP. Activation of the Akt-related cytokine-independent survival kinase requires interaction of its phox domain with endosomal phosphatidylinositol 3-phosphate. Proceedings of the National Academy of Sciences of the United States of America 2001;98:12908–12913. [PubMed: 11606732]

Vivanco I, Sawyers CL. The phosphatidylinositol 3-Kinase AKT pathway in human cancer. Nat Rev Cancer 2002;2:489–501. [PubMed: 12094235]

Watton SJ, Downward J. Akt/PKB localisation and 3' phosphoinositide generation at sites of epithelial cell-matrix and cell-cell interaction. Curr Biol 1999;9:433–436. [PubMed: 10226029]

Xu J, Liao L, Qin J, Xu J, Liu D, Songyang Z. Identification of flightless-I as a substrate of the cytokine-independent survival kinase CISK/SGK3. The Journal of biological chemistry. 2009

Zeng X, Xu H, Glazer RI. Transformation of mammary epithelial cells by 3-phosphoinositide-dependent protein kinase-1 (PDK1) is associated with the induction of protein kinase Calpha. Cancer research 2002;62:3538–3543. [PubMed: 12068001]

Zhang L, Bewick M, Lafrenie RM. EGFR and ErbB2 differentially regulate Raf-1 translocation and activation. Lab Invest 2002;82:71–78. [PubMed: 11796827]

Zhao JJ, Liu Z, Wang L, Shin E, Loda MF, Roberts TM. The oncogenic properties of mutant p110alpha and p110beta phosphatidylinositol 3-kinases in human mammary epithelial cells. Proceedings of the National Academy of Sciences of the United States of America 2005;102:18443–18448. [PubMed: 16339315]

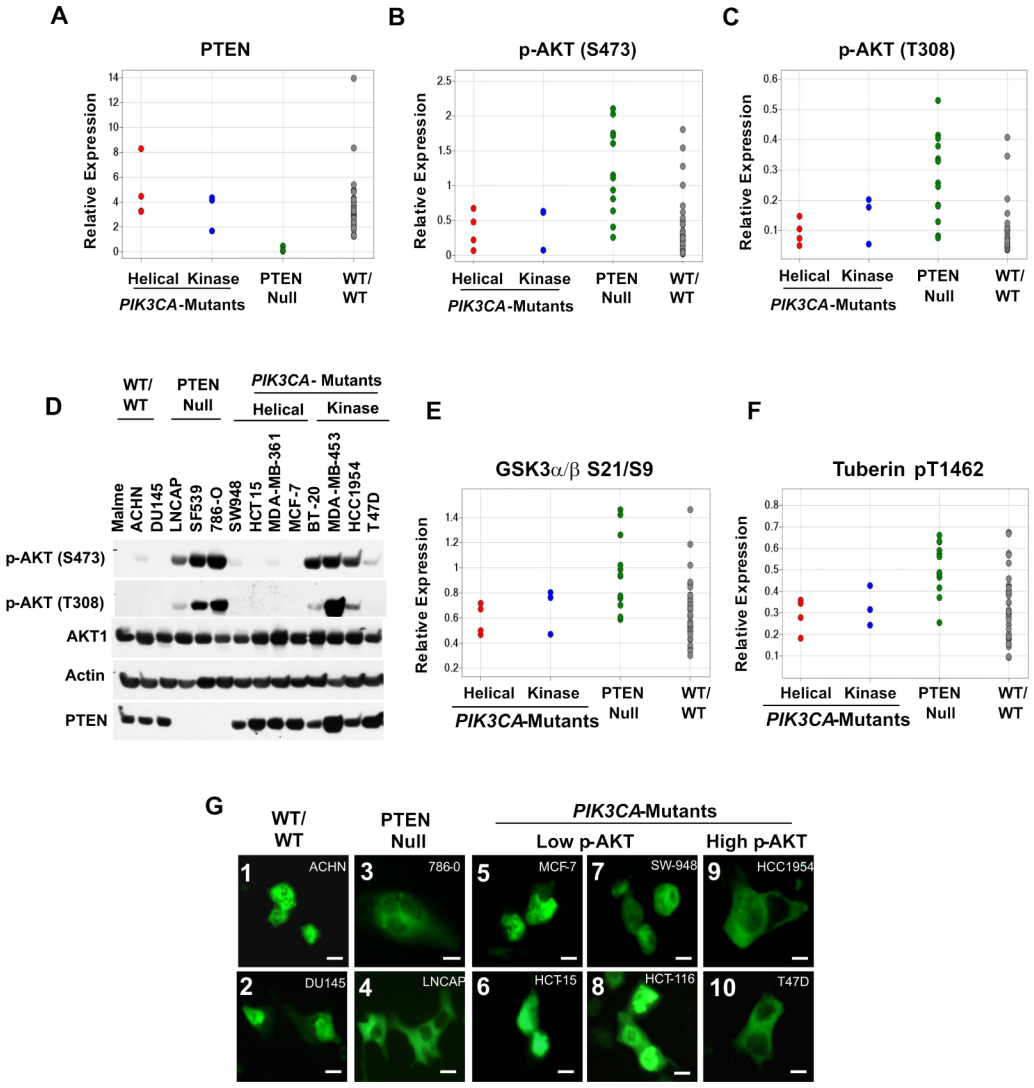

Figure 1.

PTEN-null and *PIK3CA*-mutant cancer cells show different steady-state AKT pathway activation patterns. (A-C) Quantitative RPPA protein expression levels were determined in NCI60 cells showing loss of PTEN (PTEN-null) (green), helical *PIK3CA* mutation (Helical) (red), kinase *PIK3CA* mutation (Kinase) (blue) or a wild-type pattern for PTEN and *PIK3CA* (WT/WT) (gray). Relative protein levels of PTEN (A), p-AKT (Ser473) (B) and p-AKT (Thr308) (C) are shown. The diminished PTEN protein levels in PTEN-null cells are statistically significant ($p < 0.001$ when compared to both *PIK3CA*-mutant and "wild type" cells). PTEN-null cell lines have higher p-AKT (Ser473) and p-AKT (Thr308) levels than *PIK3CA*-mutant lines ($p = 0.0006$ and $p = 0.002$, respectively) or WT/WT lines ($p = 0.0002$ and $p = 0.0003$, respectively). The *PIK3CA*-mutant cell lines do not differ significantly from the WT/WT cell lines ($p = 0.62$ and $p = 0.25$, respectively, for each p-AKT residue). (D) Immunoblot analysis of AKT phosphorylation (p-AKT) at Ser473 and Thr308 across a panel of PTEN-null or *PIK3CA*-mutant cancer cell lines. (E, F) Quantitative RPPA levels were also determined for p-GSK3-α/β (E) p-Tuberin and (F). PTEN-null cells show higher phosphorylation of both AKT substrates than *PIK3CA*-mutant cells ($p = 0.003$ and $p = 0.002$, respectively) and WT/WT lines ($p = 0.003$ and 0.001, respectively). (G) Fluorescence

microscopy of transient GFP-FOXO1 expression in PTEN-null or *PIK3CA*-mutant cancer cell lines. Lines with high p-AKT or low p-AKT are indicated. Scale bars = 30 μM.

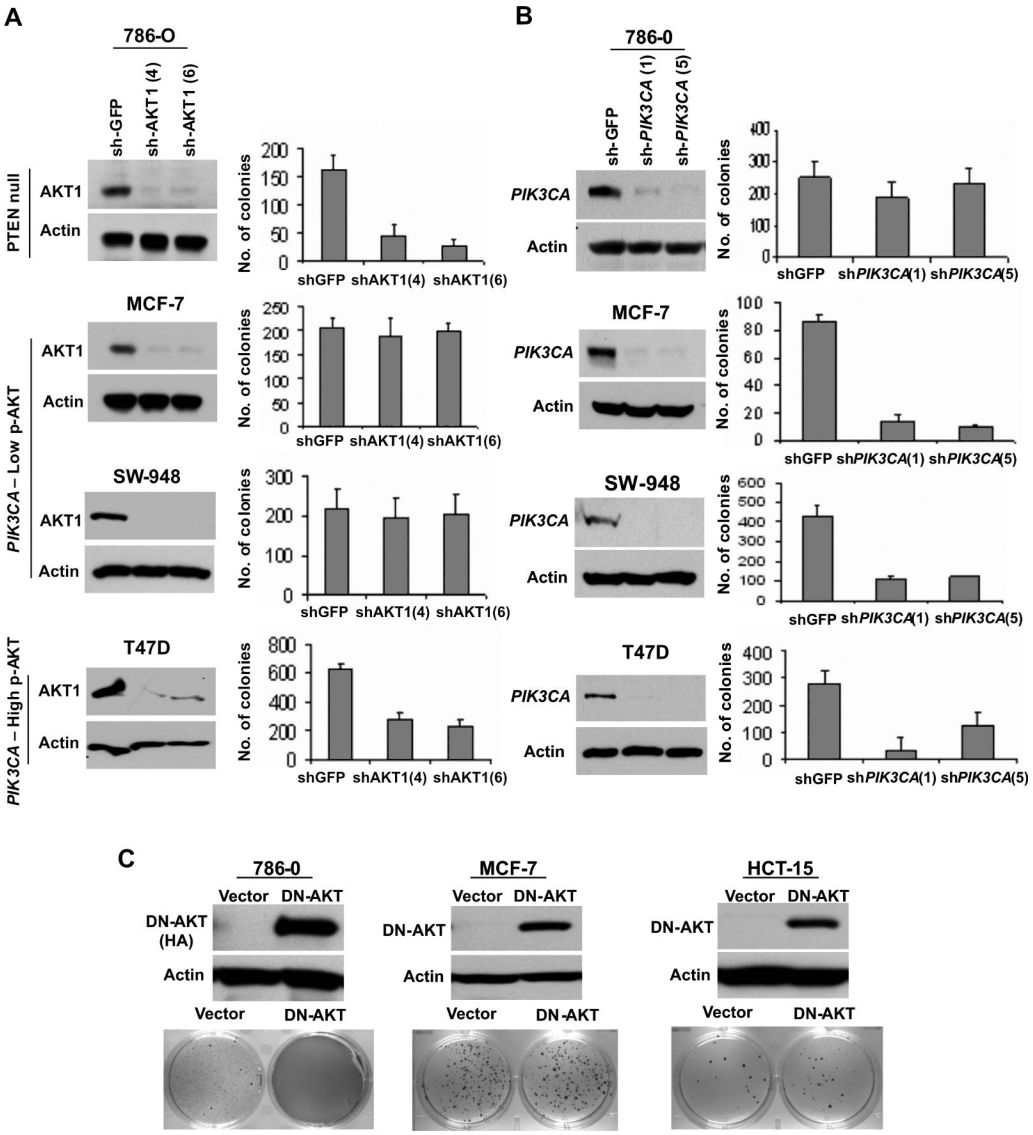

Figure 2.

PTEN-null and *PIK3CA*-mutant cells show differential dependency on AKT for cell viability and anchorage-independent growth. (A, B) Anchorage-independent growth following lentiviral RNAi knockdown of *AKT1* (A) or *PIK3CA* (B) in PTEN-null (786−0), *PIK3CA*-mutant cells with low p-AKT (MCF-7 and SW-948) and *PIK3CA*-mutant cells with high p-AKT (T47D). For each gene, knockdown efficacy of two independent shRNAs was measured by Western blot (left), and colony formation in soft agar was enumerated (right). Data are mean +/− SD; each experiment was performed in triplicate. (C) Expression of HA-tagged dominant negative AKT (DN-AKT) in PTEN-null (786−0), or *PIK3CA*-mutant cells with low p-AKT (MCF-7 and HCT15). Immunoblot analysis for DN-AKT expression (top) and effects of DN-AKT on anchorage-independent growth (bottom) are shown.

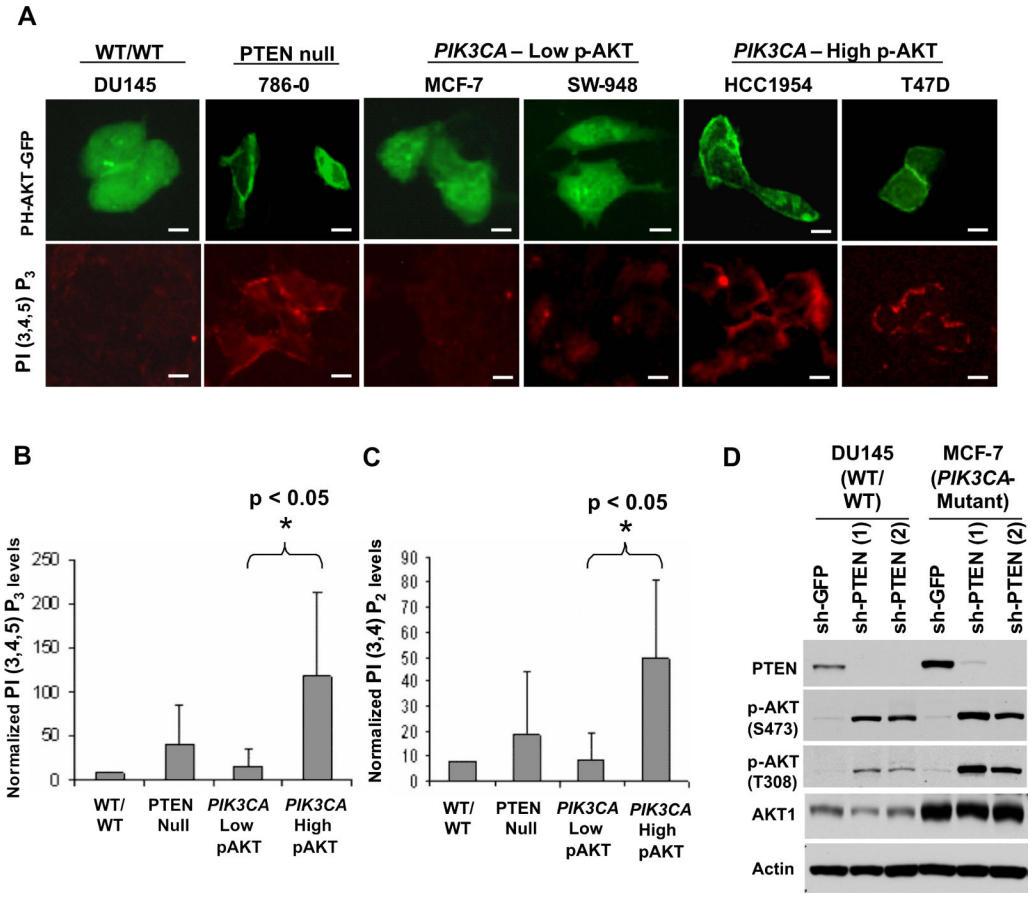

Figure 3.

AKT subcellular localization, phosphatidylinositide studies, and PTEN regulation in PIK3CA-mutant cells. (A) Immunofluorescence studies of transient PH-AKT-GFP expression (top panel) and PI(3,4,5)P_3 levels (bottom panel), and are shown for "wild-type" (DU145), PTEN-null (786−0), *PIK3CA*-mutant cells with low p-AKT (MCF-7 and SW-948) and *PIK3CA*-mutant cells with high p-AKT (HCC1954 and T47D). Scale bars = 30 μM. (B, C) Relative levels of PtdIns(3,4,5)P_3 (B) and PtdIns(3,4)P_2 (C) are shown in "wild-type" (DU145), PTEN-null (786−0 and SF-539), *PIK3CA*-mutant cells with low p-AKT (MCF-7, HCT-15 and SW-948) and *PIK3CA*-mutant cells with high p-AKT (HCC1954, MDA-MB453 and T47D). Error bars represent standard deviations of the mean for each cell line group. (D) Immunoblot analysis of AKT phosphorylation (p-AKT) at Ser473 and Thr308 following PTEN knockdown in "wild-type" (DU145) or PIK3CA-mutant cells (MCF-7).

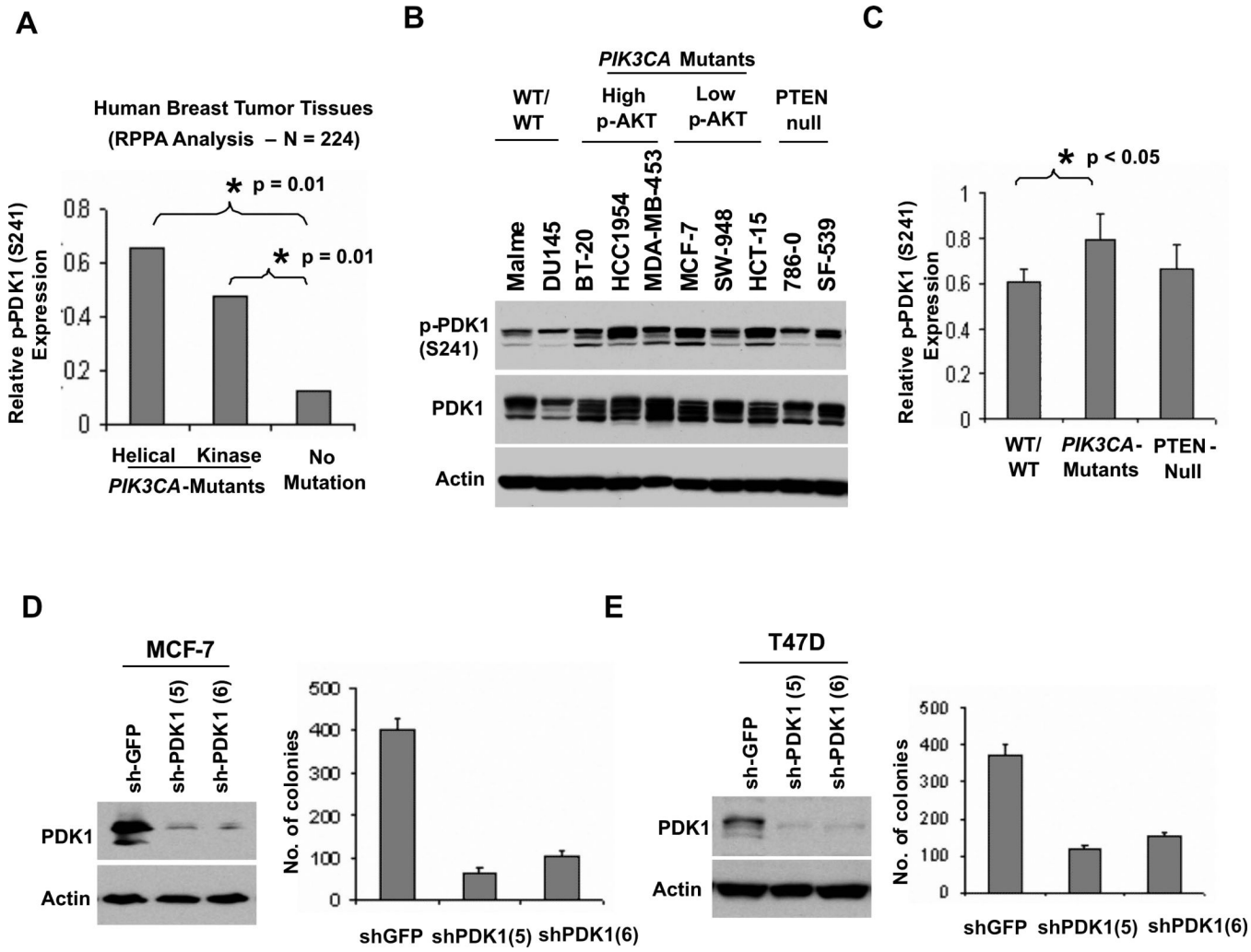

Figure 4.

PDK1-dependent signaling and tumorigenicity in *PIK3CA*-mutant cells. (A) RPPA expression of phospho-PDK1 (S241) in 224 hormone receptor positive human breast tumors. Samples were grouped according to the type of *PIK3CA* mutation (helical or kinase) or "no mutation." (B) Immunoblotting studies of phospho-PDK1 (S241) and total PDK1 are shown in "wild-type" (MALME and DU145), $PIK3CA^{helical}$ (MCF-7, SW-948, HCT-15), $PIK3CA^{kinase}$ (BT-20, HCC-1954, MDA-MB-453), and PTEN-null cells (786−0, SF-539). (C) Quantification of the immunoblot signal as average intensities + SD are shown for the cell lines in (B) above. (D, E) Anchorage-independent growth following lentiviral RNAi knockdown of *PDK1* in *PIK3CA*-mutant cells with low p-AKT (MCF-7) (D) or high p-AKT (T47D) (E). Knockdown efficacy of two independent shRNAs was measured by Western blot (left), and colony formation in soft agar was enumerated (right). Data are mean +/− SD; each experiment was performed in triplicate.

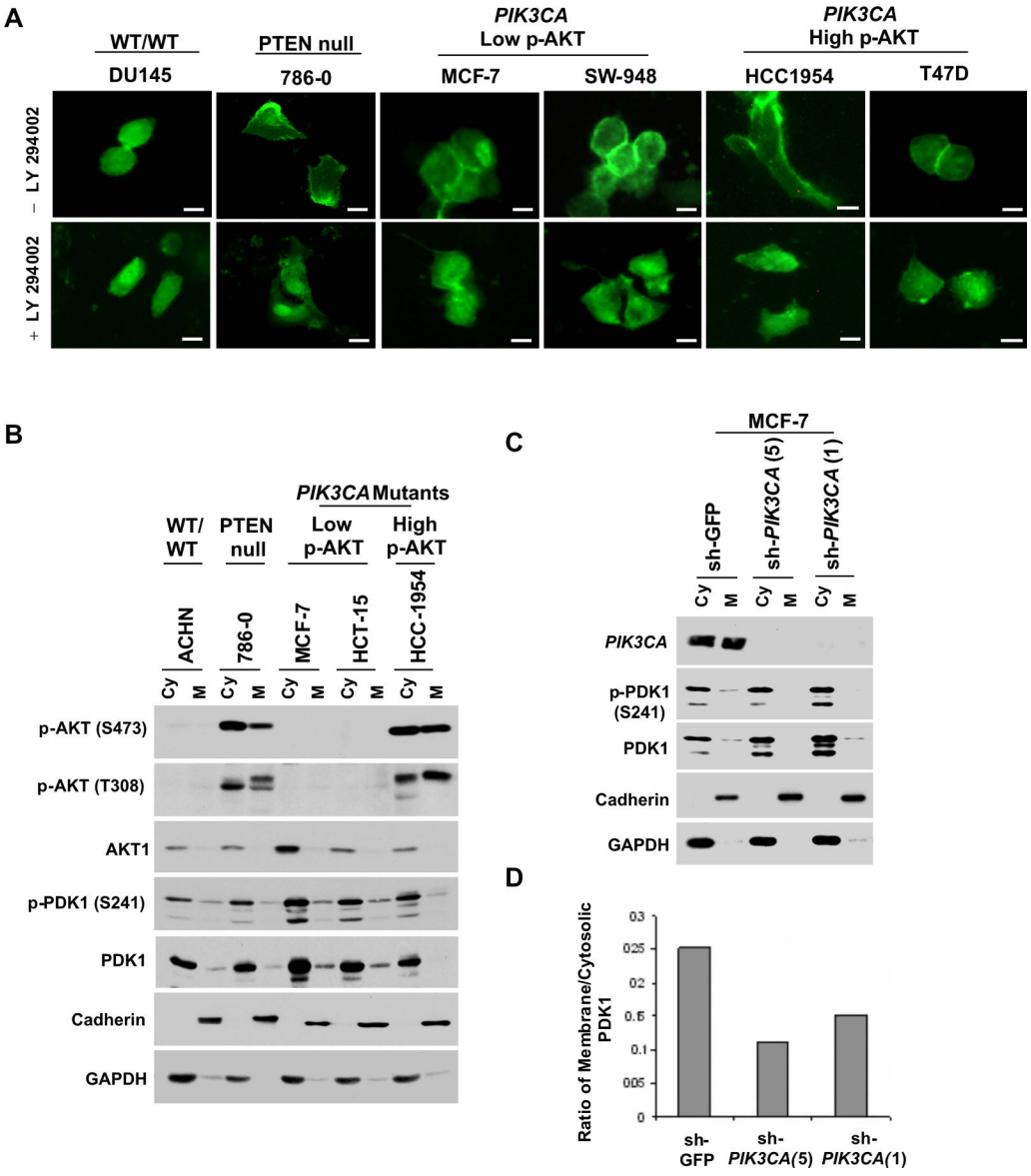

Figure 5.

PI3K-dependent membrane association of PDK1 in *PIK3CA*-mutant cells. (A) Fluorescence microscopy of transient PH-PDK1-GFP expression is shown for serum-starved "wild-type" (DU145), PTEN-null (786−0), *PIK3CA*-mutant cells with low p-AKT (MCF-7 and SW-948) and *PIK3CA*-mutant cells with high p-AKT (HCC1954 and T47D). Scale bars = 30 μM. (B) Immunoblotting studies of cytosolic (Cy) and membrane (M) fractions prepared from serum-starved "wild-type" (ACHN), PTEN-null (786−0), or *PIK3CA*–mutant cells (MCF-7, HCT-15, and HCC-1954) are shown. (C) Immunoblotting studies of cytosolic (Cy) and membrane (M) fractions prepared following shRNA knockdown of p110α (sh-*PIK3CA*) or control (sh-GFP) in serum-starved MCF-7 cells. (For (B) and (C), Antibodies recognizing p-AKT (S473), AKT1, p-PDK1 (S241), PDK1, Cadherin and GAPDH were used.) (D) Quantification of the immunoblot signal is shown as a normalized ratio of membrane/cytosolic PDK1 (total) for the blot in (C) above.

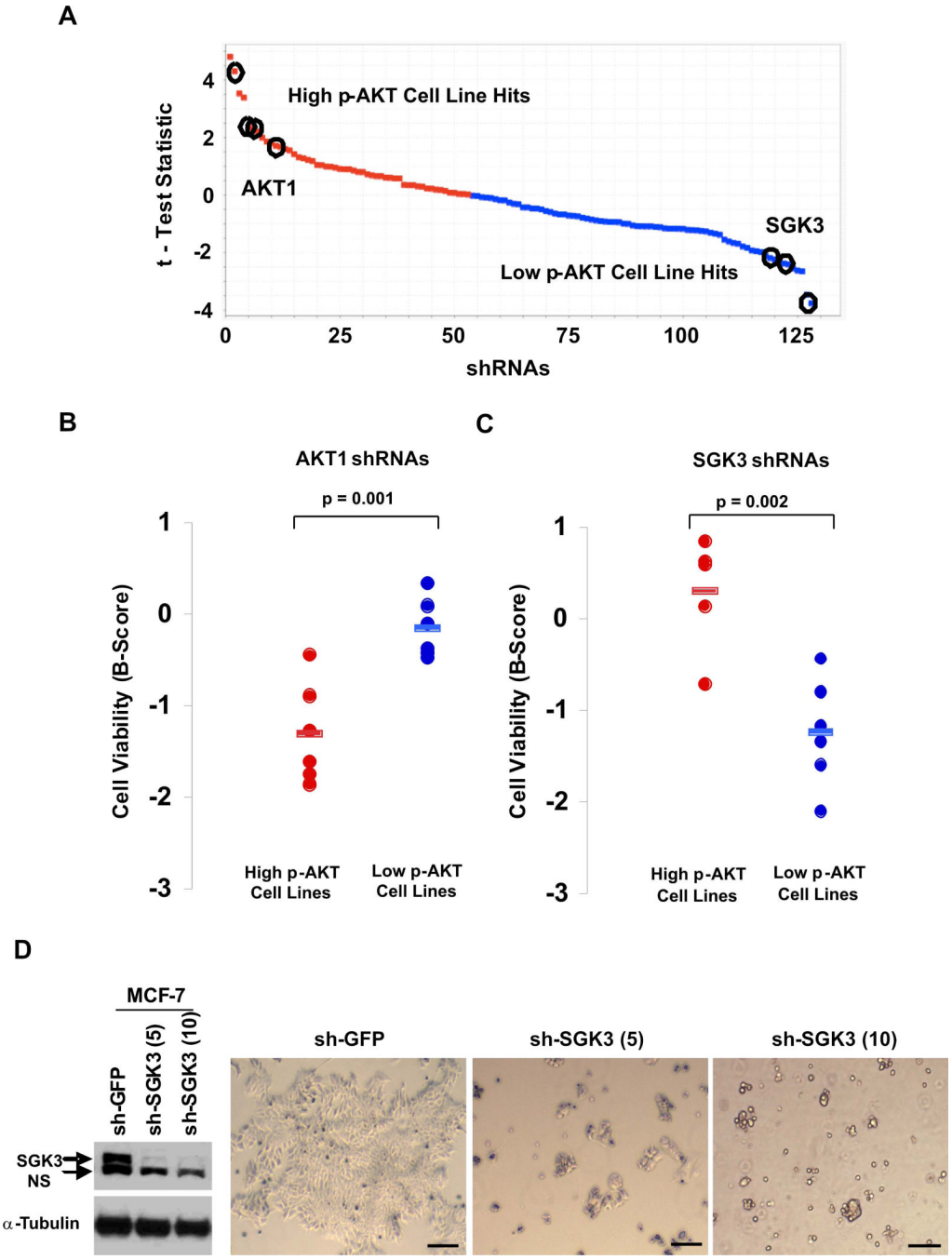

Figure 6.

SGK3 transduces an AKT-independent signal in *PIK3CA*-mutant cells. (A) Distribution of 120 hairpins against 20 PDK1 substrates ranked according to the t-test statistics applied to cell viability data. The tails of the curve represent hairpins that are selectively lethal in 3 *PIK3CA*-mutant cell lines with high p-AKT (red) compared to 3 *PIK3CA*-mutant cell lines with low p-AKT (blue). Multiple hairpins targeting *AKT1* or *SGK3* in the top 10% of hairpins distinguishing each class are indicated (circles). (B,C) Cell viability data is shown for the top-scoring, knockdown-validated *AKT1* hairpins (B) and *SGK3* hairpins (C) in *PIK3CA*-mutant lines with high vs. low p-AKT levels. (D) SGK3 expression by immunoblot analysis (left panel)

and cell viability (right panel) following lentiviral RNAi knockdown of *SGK3* in MCF-7 cells (*PIK3CA*-mutant, low p-AKT) (NS: non-specific band). Scale bars = 500 μM.

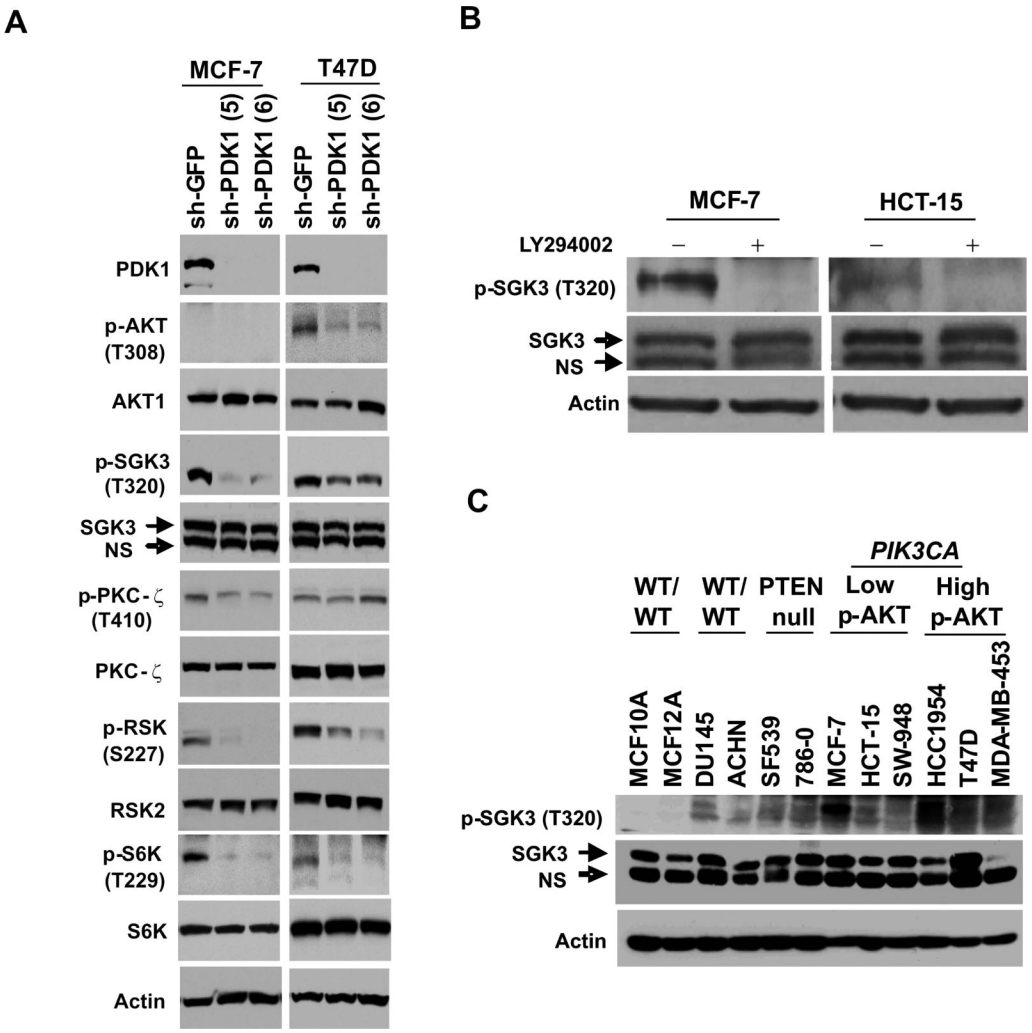

Figure 7.

(A) Immunoblot analysis of MCF-7 (*PIK3CA*-mutant, low p-AKT) and T47D cells (*PIK3CA*-mutant, high p-AKT) stably expressing shRNAs against GFP (control) or PDK1. Antibodies recognizing phospho-AKT (T308), AKT1, phospho-SGK3 (T320), SGK3, phospho-PKC ζ (T410), PKC ζ, phospho-RSK (S227), RSK2, phospho-p70 S6 kinase (T229), p70 S6 kinase, and actin were used. (B) Immunoblot analysis of SGK3 phosphorylation at Thr320 (p-SGK3(T320)) in the absence or presence of LY294002 is shown for MCF-7 and HCT-15 cells (*PIK3CA*-mutant, low p-AKT). (C) Immunoblot analysis of SGK3 phosphorylation (p-SGK3(T320)) across a panel of PI3K pathway "wild-type", PTEN-null or *PIK3CA*-mutant cancer cell lines. Non-transformed lines (MCF-10A and MCF-12A) are included as negative controls (NS: non-specific band).